On the importance of phenology in the evaporative process of the Miombo Woodland: Could it be why satellite-based evaporation estimates differ?

*Henry Zimba[1,2], Miriam Coenders-Gerrits[1], Kawawa Banda[3], Petra Hulsman[4], Nick van de Giesen[1], Imasiku Nyambe[3], Hubert. H. G. Savenije[1].

[1] Delft University of Technology, Water Resources Section, Building 23 (Faculty of Civil Engineering and Geosciences) 2628 CN Delft, P.O Box 5048 2600 GA Delft, The Netherlands.

[2] Ministry of Agriculture, Department of Agriculture, P.O Box 50595, Mulungushi House, Independence Avenue, Lusaka, Zambia.

[3] University of Zambia, Integrated Water Resources Management Centre, Department of Geology, School of Mines, Great East Road Campus, Lusaka, Zambia.

[4] Ghent University, Hydro-Climate Extremes Lab (H-CEL), Coupure links 653, 9000 Ghent, Belgium

*Corresponding author: Henry Zimba (h.m.zimba@tudelft.nl)

Abstract

Complex African ecosystems such as the Miombo Woodland, with unique plant phenology, have evaporation dynamics that have not been investigated due to very few, if at all existent, flux tower observations. Furthermore, significant differences have been observed in satellite-based evaporation estimates in the Miombo Woodland especially in the dry season. Therefore, deciding which sattelite evaporation product to use in this ecosystem is difficult, as these products vary in many respects. In this study, the actual evaporation estimates for six satellite-based evaporation estimates are compared across Miombo Woodland phenophases in the Luangwa Basin, in southern Africa. In the absence of basin scale field observations, the actual evaporation estimated using the general water balance is used as reference, to which the six satellite-based evaporation estimates have been compared. Our results show significant variation in actual evaporation estimates in the water limited, high temperature and lower forest canopy cover and leaf chlorophyll conditions in the dormant phenophase. Lowest variation is observed in water abundant, high temperature, high leaf chlorophyll content and high forest canopy cover in the maturity/peak phenophase(s). Compared to the basin scale water balance actual evaporation, all six satellite-based evaporation estimates appear to underestimate evaporation. The results of underestimation at basin scale agrees with local field observations in a dense Miombo Woodland in the Luangwa Basin, which indicates that satellite-based evaporation estimates generally underestimate dry season (dormant phenophase) and early rain season (green-up phenophase) actual evaporation. The discrepancies in dry season satellite-based evaporation estimates may be cuased by the Miombo Woodland species' phenological adaptation attributes such as: leaf fall, leaf flush, access to deep soil moisture and the within vegetation water storage, coupled with heterogenous plant species response to phenological stimuli. Therefore, it appears that satellite-based evaporation estimates using model structure, processes and inputs that are capable of capturing Miombo species dry season phenological interaction with climate are likely to have actual evaporation estimates closer to field conditions.

1 Introduction

"Vegetation phenology" refers to the periodic biological life cycle events of plants, such as leaf flushing and senescence, and corresponding temporal changes in vegetation canopy cover (Stökli *et al.,* 2011; Cleland *et al.*, 2007). Plant phenology and climate are highly congruent (Pereira *et al.,* 2022; Niu *et al.*, 2013; Cleland *et al.,* 2007). Forest plant phenological responses to trigger elements, such as temperature, hydrological and day light regimes, include among others leaf fall and leaf flush, budburst, flowering and variation in photosynthetic activity due to changes in chlorophyll levels (Pereira *et al.,* 2022; Niu *et al.*, 2013; Cleland *et al.,* 2007). The phenological responses are species-dependent and are controlled by adapted physiological properties (i.e., Lu *et al*., 2006). Plant phenology controls the access to critical soil resources such as nutrients and water (Nord and Lynch,2009). The phenological response influences plant canopy cover and affects plant-water interactions. For instance, the phenophases associated variations in canopy leaf display, i.e., due to leaf fall and leaf flush, influences how much radiation is intercepted by plants (Shahidan, Salleh, and Mustafa, 2007). Intercepted radiation influences canopy conductance. In water limited conditions, at both individual species and forest scales, leaf fall reduces canopy radiation interception while leaf flush and the consequent increase in canopy cover increases canopy radiation interception leading to increased transpiration (Snyder and Spano, 2013) controlled by available moisture storage, both vegetative and root zone. Canopy cover and its interactions with atmosphere carbon dioxide through the photosynthetic and autotrophic respiration processes influences transpiration. Ultimately, plant phenological response to changes in the trigger elements influences forest transpiration and total evaporation (i.e., Marchesini *et al.,* 2015).

Evaporation in forested land surfaces accounts for a significant portion of the water cycle over the terrestrial land mass (Sheil, 2018; Van Der Ent *et al*., 2014; Gerrits, 2010; Van Der Ent *et al*., 2010). Miralles *et al.* (2020) defined evaporation as "the phenomenon by which a substance is converted from its liquid into its vapour phase, independently of where it lies in nature". Likewise, instead of the often-used term 'evapotranspiration', in this paper the term evaporation is used for all forms of terrestrial evaporation, including transpiration by leaves, evaporation from intercepted rainfall by vegetation and forest floor, soil evaporation, and evaporation from stagnant open water and pools (Miralles *et al.,* 2020; Savenije, 2004). Understanding the characteristics of evaporation, such as interception and transpiration, in various forest ecosystems is key to monitoring the climate impact on forest ecosystems, for hydrological modelling and the management of water resources at various scales (Kleine *et al.,* 2021; Bonnesoeur *et al.,* 2019; Roberts, (n.d.)). One of the key aspects to enable this understanding is the knowledge of the forest phenological interaction with climate variables and seasonal environmental regimes (i.e., Zhao *et al.,* 2013). Plant phenology influence environmental variables differently across the diverse ecosystems globally (Forrest *et al.,* 2010; Forrest & Miller-Rushing, 2010; Kramer *et al.,* 2000) therefore requiring better understanding at a local or regional level with minimal variations. Yet, evaporation of natural forests, especially in African ecosystems, with respect to phenological phases are poorly characterised. This is largely because the development of measuring instruments and models has mainly focused on understanding the phenological response of agricultural crops to climate variables and seasons. Furthermore, phenological studies have mainly focused on mid-latitude regions which excludes other regions such as Africa (Snyder *et al*., 2013; Schwartz, 2013). It is important to account for forest phenology interaction with climate variables and seasons when characterizing evaporation in forests. This is because, for instance, accounting for phenological phases in evaporation models increases the predictive power (i.e., Forster *et al*., 2022).

The Miombo is a heterogeneous woodland with a unique and complex phenology adapted
to dry season conditions such as leaf shedding, deep rooting with access to ground water resources,
and vegetation (i.e., stem) water storage (Vinya *et al.,* 2018; Tian *et al.,* 2018; Guan *et al.*, 2014;
Chidumayo, 2001; Frost, 1996; Fuller, 1996). Leaf flushing alos occurs before the commencement
of seasonal rainfall (Chidumayo, 1994; Fuller and Prince, 1996). While at individual species level
the entire tree canopy can be leafless or changing leaf colour this does not occur at forest canopy
level due to heterogeneity in species composition and varied species response to phenological
stimuli. The Miombo Woodland canopy cover varies with phenophases. These phenological
attributes influence the evaporation process (Forster *et al*., 2022; Snyder *et al*., 2013; Schwartz,
2013). There is currently no publication in the public domain showing how various satellite-based
evaporation estimates compare in the Miombo Woodland, especially with a focus on the Miombo
phenology across climatic seasons. Yet, the usage of satellite-based evaporation estimates in the
management of water resources globally and in Africa is on the increase (García *et al.*, 2016;
Zhang *et al., 2016;* Makapela, 2015). However, because of the absence or scarce field observations
and extremely limited validation, it is impossible to know which satellite-based evaporation
estimates are close to actual physical conditions of the Miombo ecosystem. In most cases, the
choice for a satellite-based evaporation product is based on validation results in non-Miombo
ecosystems. This product choice scenario is a challenge in that non-Miombo ecosystems have a
different phenology and evaporation to that of the Miombo ecosystem. For instance, a satellite
evaporation product that performs extremely well in energy limited conditions and homogeneous
forests, e.g., in Europe, cannot be assumed to have the same performance in a warm, water limiting
and heterogeneous forest such as the Miombo.

Therefore, this study was formulated in order to contribute to the bridging of the gap in
information on satellite-based evaporation estimates performance in different phenophases of the
Miombo Woodland. We focused on the Luangwa sub-basin in the larger Zambezi Basin, one of
the largest river basins in the Miombo ecosystem. The Luangwa Basin was chosen because it is
situated in a sparsely gauged region (Beilfuss, 2012), where it is essential that management of
water resources is based on reliable information, for various competing uses, i.e. hydropower,
agriculture, wildlife, industrial and domestic (WARMA, 2022). The Luangwa Basin also falls in
both dry (i.e., southern Miombo Woodlands) and wet (i.e., central Zambezian Miombo
Woodlands) Miombo. The central Zambezian Miombo is the largest of the four Miombo sub-
groups, the other three being the Angolan Miombo, Eastern Miombo, and the Southern Miombo
(Frost, 1996; White, 1983). It is also located in Zambia, argued to have the highest diversity of
Miombo Woodland trees and considered centre of endemism for the Miombo Woodlands
Brachystegia species (Frost, 1996). These attributes suggest a catchment that provides a fair
representation of the Miombo Woodlands conditions and an appropriate site for this type of study.
Therefore, the aim of this study was two-fold:

(i) Compare the temporal trend and magnitude of six satellite-based evaporation estimates
across phenophases of the Miombo Woodland.
(ii) Compare satellite-based estimates of actual evaporation with water balance-based
estimates at the Luangwa Basin scale.

2 Materials and Methods
2.1 Study approach

The study had a two-way approach. The main focus of the study was about understanding
the behaviour of satellite-based evaporation in terms of behaviour of estimates of evaporation

Hydrology and
Earth System
Sciences
Discussions
Open Access
EGU

across the different phenophases in the Miombo Woodland. This helped to observe whether the behaviour (i.e., trend and magnitude) of satellite-based evaporation estimates is in tandem with the phenology-water interaction behaviour (i.e., trend and magnitude) of the Miombo Woodland across seasons. Furthermore, point scale observations in the wet Miombo Woodland (Zimba *et al.*, 2022) showed that satellite products underestimated actual evaporation in the dry season and early

140   rain season phenophases. The question is whether this behaviour is reflected in the annual basin-scale satellite-based evaporation estimates. Therefore, to better understand which of the product(s) were closest to Miombo Woodland evaporation, the satellite products' estimates were compared with water balance estimates for the Luangwa Basin at annual scale. A 12-year period from 2009 – 2020 was used for the assessments. This period was chosen because of data availability and was sufficient to capture long-term seasonal, monthly and annual variations in catchment actual evaporation.

2.2   Classification of Miombo Woodland phenophases

Classification of the phenophases was based on the Collection 6 MODIS Land Cover

150   Dynamics (MCD12Q2) Product (Gray *et al.,* 2019), Zimba *et al.* (2020), as well as field observations of the Miombo phenology in the Luangwa Basin. Figure 1 shows the phenophases classification. The phenophases include: Green-up, Mid-Green up, Maturity, Peak, Senescence, Green-down, and Mid-green down and dormant. For ease of analysis the phenophases were merged into four groups based on dominant activity in each phase.
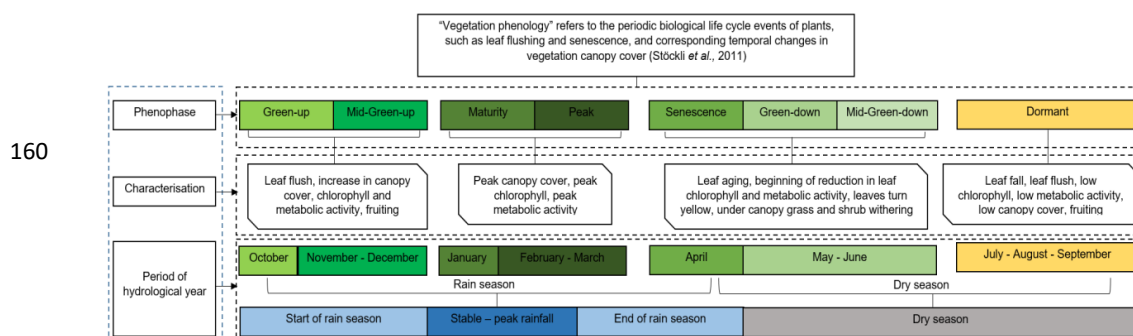
160

Figure 1. Grouping and description of phenophases in relation to seasonality for the Luangwa Basin used in the study.

170   **2.3   Delineation of the Miombo Woodland for the Luangwa Basin**

Two approaches were used for the delineation. Firstly, for phenophase-based comparison of satellite-based evaporation estimates we used the delineation of typical Miombo Woodland regions as conducted by White (1983) and the vegetation map shown in Ryan *et al.* (2016) (see Fig. 2). The delineated Luangwa Basin Miombo Woodland excluded the Mopane Woodland, Mixed Woodland as well as the large water bodies like dams. This ensured that only the areas classified as typical Miombo Woodland (Ryan *et al.*, 2016; White, 1983) were considered. The limitation with this approach is that, at the Luangwa Basin scale, what is classified as typical Miombo Woodland regions includes other land covers like water bodies, cropland, grassland and settlements/build up land. A more focused comparison was performed by using a known typical

180   Miombo Woodland land-cover with extremely limited anthropogenic activities. This was

conducted in order to put the basin boundary Miombo Woodland generalisation into context. The area of focus was based on approximately 27.7 km by 27.7 km grid of the coarsest resolution of the satellite-based evaporation estimates used in the study. The comparison was aimed at observing the extent of variations in satellite-based evaporation estimates in different Miombo Woodland phenophases. Secondly, comparison of satellite-based evaporation estimates with the water balance estimates was conducted using the entire Luangwa Basin boundary. This is because the observed run-off data is generated from the entire Luangwa Basin including non-Miombo regions. The comparison was aimed at establishing whether satellite-based evaporation estimates underestimate or overestimate evaporation in a largely Miombo Woodland basin.

190

2.4   Satellite-based evaporation estimates used in the study

Compared to other ecosystems, Pelletier *et al.* (2018) and Tian *et al.* (2018) observed that Miombo Woodland species exhibit distinct behaviour (i.e., forest canopy display and the vegetation water content) during the dry season. To this effect this study compared the behaviour (i.e., trend and magnitude) of six satellite-based evaporation estimates across the Miombo Woodland phenophases with emphasis on the dry season. This was conducted in order to observe existence of discrepancies in monthly temporal behaviour of satellite-based evaporation estimates under changing seasons and phenological stages. The six satellite-based evaporation estimates consisted of: 1) FLEX-Topo (Hulsman *et al.,* 2021; Hulsman *et al.,* 2020; Savenije, 2010); 2)

200   Thornthwaite-Mather Climatic water balance model (TerraClimate) (Abatzoglou *et al.,* 2018); 3) Global Land Evaporation Amsterdam Model (GLEAM) (Martens *et al.,* 2017; Miralles *et al.,* 2011); 4) Moderate-resolution Imaging Spectrometer (MODIS) MOD16) (Running *et al.,* 2019; Mu *et al.,* 2011; Mu *et al.,* 2007); 5) Operational Simplified Surface Energy Balance (SSEBop) (Savoca *et al.,* 2013) and 6) Water Productivity through Open access of Remotely sensed derived data (WaPOR) (FAO, 2018). These products were selected purely because they are free of charge and easily accessible from various platforms, and have an archive of historical data with appropriate temporal and spatial resolutions. Furthermore, excluding FLEX-Topo, the other five satellite-based estimates cover the entire Miombo Woodland of Africa. Except for FLEX-Topo and GLEAM (with spatial resolution of 27.7 km), these products have high spatial resolution (i.e.,

210   500 m, 1000 m, 4000 m and 250 m for MOD16, SSEBop, TerraClimate and WaPOR respectively) and temporal resolution (daily, 8-day, dekadal and monthly respectively), which attributes were deemed suitable for this study. The original spatial resolutions of the six evaporation estimates were used. This was because these products are normally applied as is, in their original resolutions. Resampling the spatial resolutions to a standard resolution was thought to be problematic as it would have introduced unknown and unquantifiable errors, regardless the extent resampled.

2.5 Basin water balance –based evaporation

In cases where spatially distributed measurements are not available, as is the case with large basins and more importantly in the Luangwa Basin, the use of the water balance approach is

220   an acceptable approach (i.e., Weerasinghe *et al.,* 2020; Liu *et al.,* 2016). The general basin annual average water balance evaporation (E_{wb}) is estimated using Eq. (1) where over-year storage change is neglected.

$$E_{wb} = P - Q \tag{1}$$

Hydrology and
Earth System
Sciences
Discussions

Open Access

EGU

Where, P is the annual average catchment precipitation in mm year^{-1} and Q is annual average discharge in mm year^{-1}. The precipitation and discharge information for the water balance approach were selected and used as explained below.

230 ## 2.6   Precipitation products

The challenge posed by using satellite precipitation data in African catchments is that most, if not all, satellite precipitation products are geographically biased towards either underestimation or overestimation, despite some of them having good correlation with ground observations (i.e., Macharia *et al.,* 2022; Asadullah *et al.*, 2008; Dinku *et al.,* 2007). The lack of adequate ground precipitation observations makes it difficult to validate, as well as correct, the product(s') biases with a good degree of certainty. There is not a single precipitation product that can be said to perform better across African landscapes and southern Africa in particular (i.e., Macharia *et al.,* 2022). There is no guarantee any of the precipitation products are spatially representative of a basin that is about 159,000 square kilometres with varying topographical attributes. Using an ensemble 240 of precipitation products is said to reduce errors and therefore, recommended (i.e., Asadullah *et al.*, 2008). To this extent, for the general water balance, this study used annual mean of four satellite precipitation products. The four precipitation products are the Climate Forecasting System Reanalysis (CFSR), Climate Hazards Group Infra-Red Precipitation with Station data (CHIRPS), ECMWF Reanalysis v5 (ERA5) and TerraClimate. These products were selected purely based on availability and the fact that they had desirable spatial and temporal resolutions.

2.7   Runoff data

The linear regression approach, with the 1981-1990 field observations and TerraClimate run-off data, was used to extend the run-off time series for the period 2009 - 2020. This was 250 performed because reliable field observations of runoff were only available for the period 1981 – 1990. The TerraClimate data was used because of availability free of cost and with relatively fine temporal and spatial resolution (monthly and 5 km respectively). Generally, both observed and extended (with TerraClimate data) annual runoff was, on average, 11 percent of annual satellite-based precipitation. With the given assumptions it was deemed that the satellite precipitation and run-off products used were adequate for the study.

2.8   Field observations of forest canopy phenology

To observe changes in canopy cover in the Miombo forest, a Denver digital camera was installed on a tower above the canopy of a known Miombo Woodland in Mpika (Fig. 2). This was 260 conducted to obtain field imagery to compare with the temporal behaviour of satellite-based leaf area index (LAI) and the normalised difference vegetation index (NDVI), and the satellite evaporation product's behaviour across phenophases. In addition, the fish eye lens was used to obtain images of differences in canopy leaf fall among Miombo species. The observations were conducted for the period January – December 2021.

2.9   Statistical analyses

The coefficient of variation C_v (%) in Eq. (2) (Helsel *et al.,* 2020) was used to understand the extent to which the satellite-based evaporation estimates varied among each other across phenophases. Correlation among satellite-based evaporation estimates was assessed at monthly 270 and annual scales using the Kendal correlation test (Helsel *et al.,* 2020). To establish the extent to

which the satellite-based evaporation estimates underestimated or overestimated evaporation, relative to E_{wb}, the mean bias (Eq. 3) was used.

$$C_v = \frac{\sigma}{\mu} \qquad (2)$$

Where σ is the standard deviation and μ is the mean of the observations. The higher the C_v value, the larger the standard deviation compared to the mean, which implies greater variation among the variables.

280     $$\text{MeanBias} = \sum(X - \acute{Y})/N \qquad (3)$$

Where N = number of observations, $\acute{Y}$ = actual observations time series and X is the modelled time series. The smaller the mean bias value (positive or negative), the less the deviation of the predicted values from the observed values (Helsel *et al.,* 2020).

2.10   Data sources

Sources and characteristics of the data used in this study are shown in Table 1. The FLEX-Topo was included because it was structured for the Luangwa Basin landscape and was calibrated on field-based discharge of the basin at a daily scale (Hulsman *et al.,* 2021). The FLEX-Topo

290   model is forced with spatially distributed CHIRPS precipitation and GLEAM potential evaporation. Each cell has been discretised into functionally distinct hydrological response units (HRU) based on the topography. The model uses a single ground water system within a grid cell to which all HRUs are connected. The model is composed of several storage components representing the interception storage, unsaturated root-zone storage, as well as fast and slow responding storages. Furthermore, each storage component has been structured as a reservoir with matching water balance equations. In terms of performance, with respect to observed discharge, calibrated for the period 2004 -2009, the model performed relatively well with the following Nash-Sutcliffe metrics: NS_Q = 0.66 (using discharge time-series), NS_log (Q) = 0.82 (using logarithmic discharge time-series), NS_FDC = 0.91 (using flow duration curve) and NS_log

300   (FDC) = 0.97 (using logarithmic flow duration curve). However, the limitation with the FLEX-Topo was the 27.7 km spatial resolution. For the GLEAM, MOD16, SSEBop and WaPOR the detailed explanations on the model configurations, processes and inputs are provided in the respective references as given in Table 1.

310

Table1. Characteristics of satellite products used in the study

| Variable	Product name	Time Period	Spatial coverage/Location	Temporal resolution	Spatial resolution	Reference	Source of data
Precipitation and temperature	CFSR v2	2009 - 2020	Global	Daily	19.2 km	(Saha et al., 2014; Saha et al., 2010)	Climate Engine
	CHIRPS	2009 - 2020	Global	Daily	27	(Funk et al., 2015)	Climate Engine
	ERA5	2009 - 2020	Global	Daily	24	(Hersbach et al., 2017)	Climate Engine
	TerraClimate	2009 - 2020	Global	Monthly	5 km	(Abatzoglou et al. 2018)	Climate Engine
LAI	MODIS	2021	Global	8-days	0.5 km	(Myneni & Park, 2015)	Global subsets tool: MODIS/VIIRS Land Products
NDVI	MODIS	2021	Global	8-days	0.5 km	(Didan, 2015)	Climate Engine
Runoff	Observations	1981-1990	N/A	Daily	N/A		WARMA, Zambia
	TerraClimate	2009 - 2020	Global	Monthly	5 km	(Abatzoglou et al., 2018)	Climate Engine
Net radiation	CFSR v2	2009-2020	Global	Daily	19.2 km	(Saha et al., 2014; Saha et al., 2010)	Climate Engine
Soil moisture	CFSR v2	2009-2020	Global	Daily	19.2 km	(Saha et al., 2014; Saha et al., 2010)	Climate Engine
Digital elevation model (DEM)	ASTER GDEM v3	N/A	Global	N/A	30	(Abrams and Crippen, 2019)	NASA Glovis portal
Land cover map	Copernicus CGLS-LC100 v3	2019	Global	Annual	100	(Buchhorn et al., 2020)	Google Earth Engine
Evaporation	FLEX-Topo	2009 - 2020	Catchment	Daily	27.7 km	(Hulsman et al., 2021; Hulsman et al., 2020; Savenije, 2010)	This study
	GLEAM (v3.2a)	2009 - 2020	Global	Daily	27.7 km	(Martens et al., 2017; Miralles et al., 2011)	GLEAM FTP server
	MOD16v2	2009 - 2020	Global	8-day	0.5 km	(Running et al., 2019; Mu et al., 2011)	Global subsets tool: MODIS/VIIRS Land Products; Climate Engine
	SSEBop	2009 - 2020	Global	Monthly	1 km	(Savoca et al., 2013).	Climate engine
	TerraClimate	2009 - 2020	Global	Monthly	4 km	(Abatzoglou et al., 2018)	Climate engine
	WaPOR v2. (ETLook)	2009 - 2020	Continental	Decadal	0.25 km	(FAO, 2018)	WaPOR Portal

320

330

340

350

360

2.11   Study site

The Luangwa is a sub-basin in the larger Zambezi Basin in sub-Saharan Africa in Zambia with spatial extent of about 159,000 km² (Beilfuss, 2012; World Bank, 2010). Based on the Miombo Woodland delineation by White (1983) and the vegetation map shown in Ryan *et al.* (2016) as given in Fig. 2 (a), 75 percent of the total Luangwa Basin land mass is covered by the Miombo Woodland, both dry and wet Miombo.

370
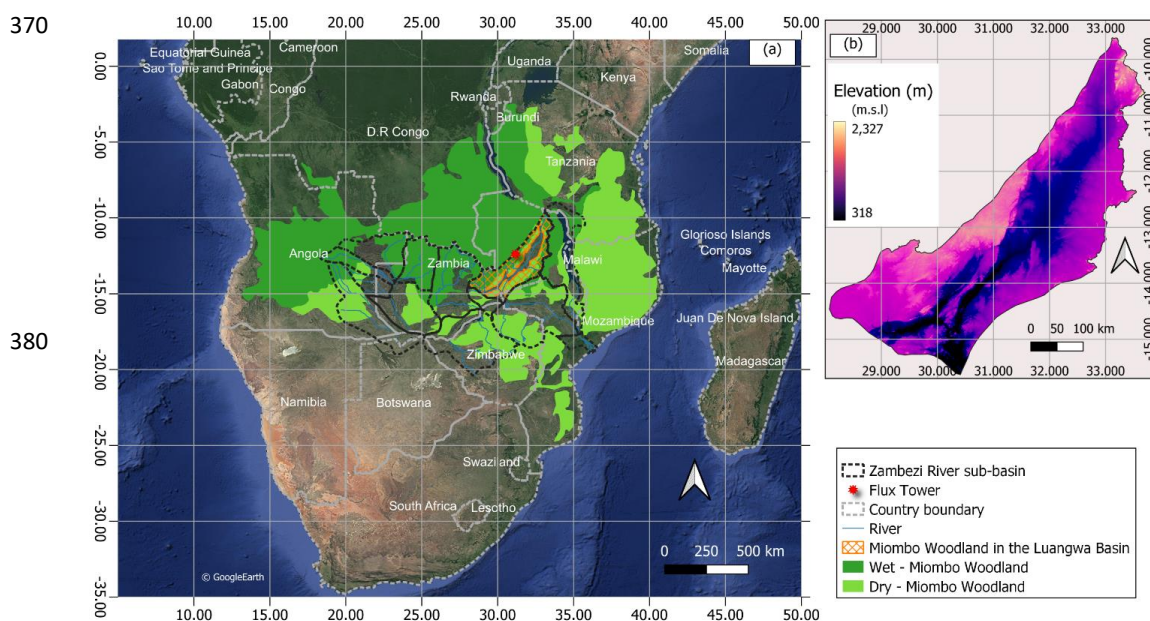
380

Figure 2. (a) Spatial extent of the Miombo Woodland in Africa and the location of the Luangwa Basin in Zambia. (b) Spatial distribution of elevation in the Luangwa Basin and the Miombo Woodland extent as illustrated by ASTER digital elevation model (DEM). Google earth satellite (©Google Earth) image as backdrop.

390

Additionally, the 2019 Copernicus land cover classification (Fig. A1 in the appendices), with 80 percent user accuracy and forest classification accuracy of about 75% (Buchhorn *et al.,* 2020; Martins *et al.,* 2020), indicates that 77 percent of the total basin area is forest (dense and open forest) which is largely Miombo Woodland.

Elevation ranges between 329 – 2210 m above mean sea level with the central part generally a valley. Miombo Woodland, both dry and wet, is generally in the upland (Fig. 2 b). The Luangwa River, 770 km long, and its tributaries drain the basin (Beilfuss, 2012). The Luangwa Basin is scarcely gauged. This has resulted in a paucity of data on various hydrological aspects such as rainfall and discharge. The basin is located in a climate environment characterised by a well-delineated wet season, from October to April and a dry season, May to October. Furthermore, the dry season is split into the cool-dry (May to August) and hot dry (August to October) seasons. The movements of the inter-tropical convergence zone (ITCZ) over Zambia between October and April dominate the rainfall activity in the basin. The basin has a mean annual precipitation of about 970 mm yr^{-1}, potential evaporation of about 1560 mm yr^{-1}, and river runoff reaches about 100 mm
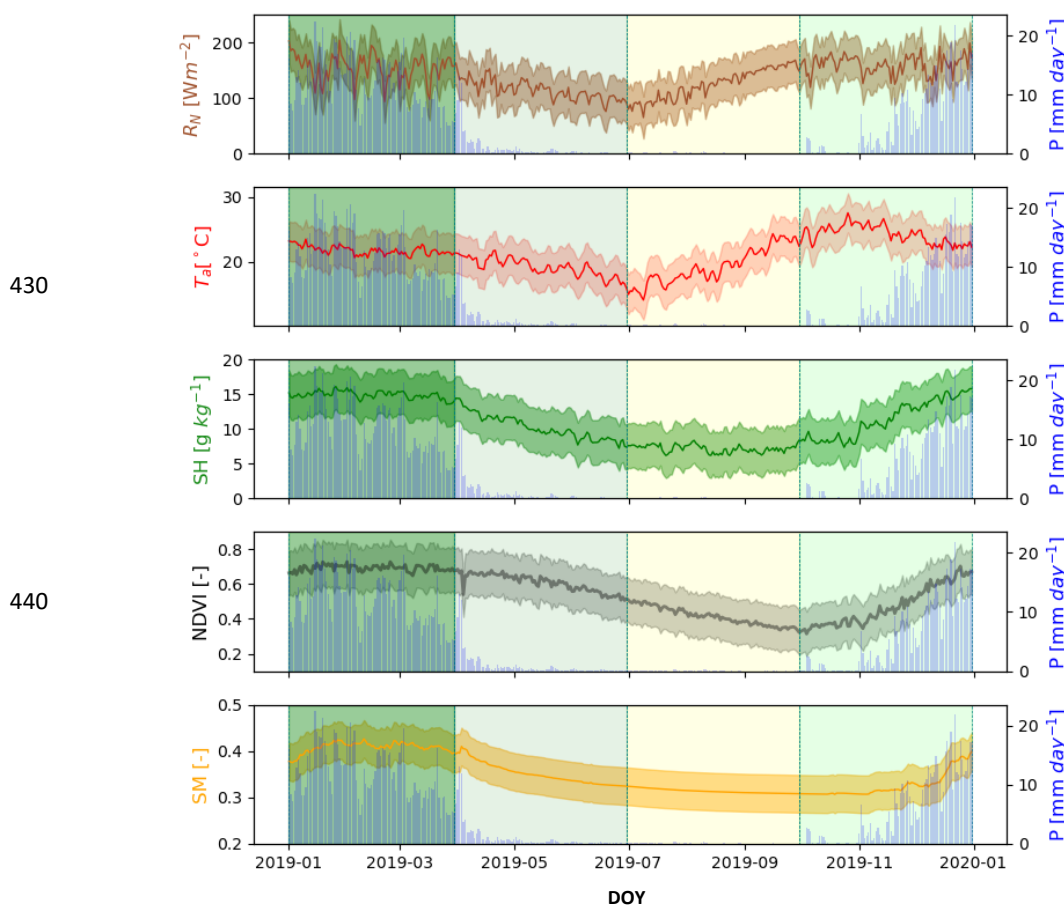
400

410   yr^{-1} (Beilfuss, 2012; World Bank, 2010). The key character of the Miombo Woodland species is that they shed off old leaves and acquire new ones during the period May to October in the dry season. Depending on the amounts of rainfall received in the preceding rain season the leaf fall and leaf flush processes may start early (i.e., in case of low rainfall received) or late (in case of high rainfall received) and may continue up to November (i.e., in the case of high rainfall received) (Frost,1996).

3   Results and discussion
3.1   Climate and phenological conditions

Figure 3 shows Luangwa Basin Miombo Woodland aggregated 2009-2020 average NDVI and CFSR data climate conditions, net radiation (R_N), air temperature (T_a), specific humidity (SH),
420   soil moisture (SM) and precipitation (P).

Figure 3. Luangwa Basin Miombo Woodland aggregated 2009-2020 daily climate and phenological conditions NDVI, (net radiation (R_N), air temperature (T_a), specific humidity (SH), soil moisture (SM) and precipitation (P). Shaded areas represent the four phenophases.

Hydrology and
Earth System
Sciences
Discussions

Open Access

EGU

In Fig. 3, the shaded areas represent the phenophases as used in this study: January – March is the peak/maturity phenophase, April – June is the senescence/Green-down phenophase, July – September is the Dormant phenophase and October – December is the green-up/mid-green-up phenophases. Shaded area for variables is the standard deviation. The NDVI was used as proxy for phenological conditions through canopy biomass formation, variations in forest canopy cover (i.e., leaf fall and leaf flush), and changes in forest canopy chlorophyll conditions (i.e., Guan *et al.,* 2014; Santin-Janin *et al.* 2009; Chidumayo, 2001; Fuller, 1999). Climate variables net radiation, air temperature, specific humidity and phenology proxy NDVI co-varied depending on the phenophase.

The peak climate and phenological variables values were generally observed in the rain season, green-up and maturity/peak phenophases. The lowest values were observed in the dry season in green-down and dormant phenophases. The relationship between climate and phenology in the Miombo Woodland generally agreed with observations made by Chidumayo (2001) and in other ecosystems (Pereira *et al.,* 2022; Niu *et al.*, 2013; Cleland *et al.,* 2007).

3.2 Comparison of satellite-based evaporation estimates across phenophases
#### 3.2.1 Delineation of Luangwa Basin and pixel level Miombo Woodland

Comparison of satellite-based evaporation estimates behaviour in the entire Luangwa Basin's Miombo Woodland was based on the delineation in Fig. 2. The delineated area excluded non-Miombo vegetation and features such as Mopane woodland, large water bodies (i.e., dams and lakes) and the grass wetlands in the middle of the basin (Fig. 2). Therefore, this comparison was based on mean estimates for the entire Luangwa Basin Miombo Woodland. The limitation with this approach is that the mean estimates included other land cover types such as cropland, settlements and grasslands. A more focused comparison at pixel scale (Fig. 4) was conducted based on a known typical Miombo Woodland in the uplands, north western side of the Luangwa Basin at Mpika. The pixel-based comparison used actual location of FLEX-Topo and GLEAM pixels with original spatial resolutions (approximately 27.7 by 27.7 km) (Fig. 4). For MOD16, SSEBop, TerraClimate and WaPOR, the mean of actual evaporation estimates in all the pixels within the dotted red square were used.

3.2.2 Comparison of temporal variations in estimates of satellite-based evaporation estimates

Figure 5 shows results for the comparison at (a) dense Miombo Woodland pixel and (b) Luangwa Basin Miombo Woodland level. Across phenophases the behaviour of satellite-based evaporation estimates at both scales appeared similar, as evidenced by the coefficients of variations (Fig. 5) and correlation coefficients (Table A1 in the appendices). Consequently, phenophase-based assessment of variations within each satellite evaporation product and across products is only shown at pixel level (Fig. 6). At pixel level the least difference among satellite-based evaporation estimates was observed in the senescence/green-down phenophase (C_v =7.83 percent) while at the Luangwa Basin level the maturity/peak showed the least difference (C_v = 6.92 percent). The maturity/peak phenophase had highest rainfall (above 190 mm/month), highest canopy cover (i.e., NDVI > 0.6), highest soil moisture and net radiation of above 150 W m^2 (Fig. 3). Lower variation and relatively higher correlation (Figs. 6 & 7 and Table A1 in the appendices) among satellite-based evaporation estimates in the maturity/peak and senescence/green-down phenophases suggests similarity in behaviour, and that it is easier to estimate Miombo evaporation in high moisture, high canopy cover and high available energy conditions.

Hydrology and
Earth System
Sciences
Discussions

Open Access

EGU
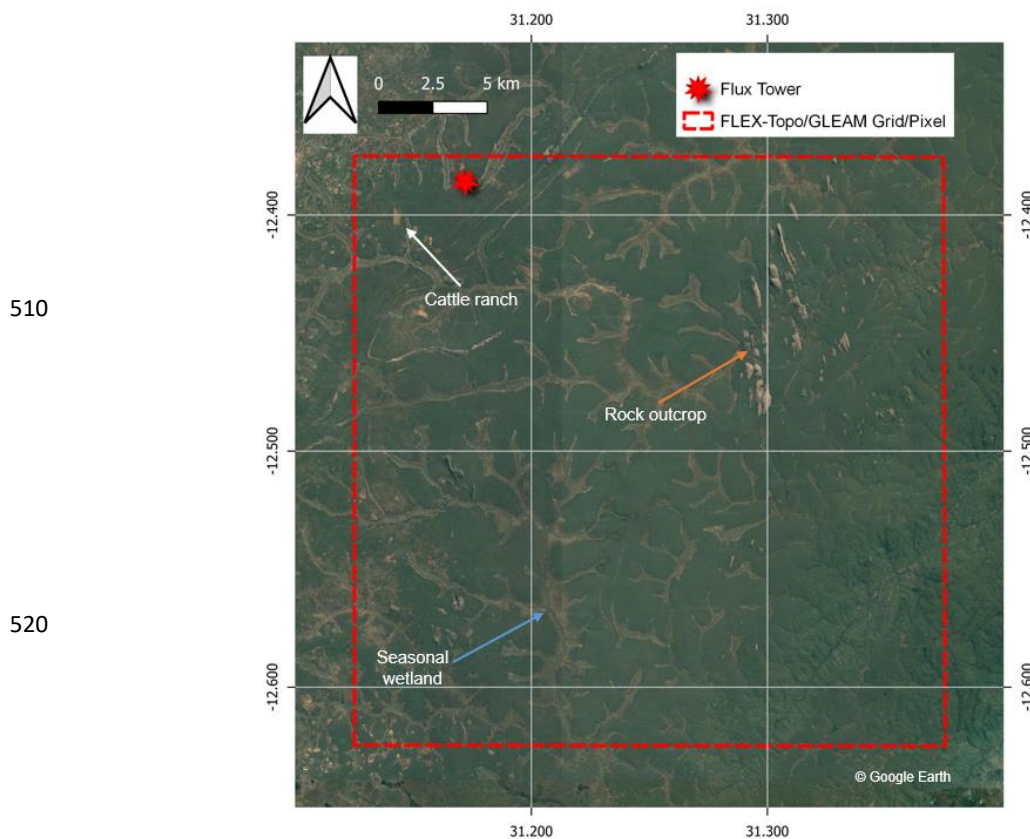
Figure 4. Typical Miombo Woodland area used for comparison of satellite products at FLEX-Topo and GLEAM spatial resolution (approximately 27.7 km by 27.7 km). The dotted red line is the actual location of the FLEX-Topo and GLEAM pixels. Seasonal wetlands are typical Miombo ecosystem features.

Significant differences in satellite-based evaporation estimates, at both pixel level in dense Miombo Woodland and at the Luangwa Basin Miombo Woodland scale, were observed during the green-up (C_v = 28.23; 22.63 percent respectively) and dormant phenophase (C_v =36.72; 39.98 percent respectively) (Fig. 5). The green-up phenophase is at the commencement of the rain season with relatively high canopy cover (i.e., mean NDVI between 0.5 and 0.7) and highest net radiation (i.e., 150 Wm^2). The dormant phenophase is during the driest part of the year with the lowest moisture in the top soil, least forest canopy cover (i.e., NDVI $\approx$ 0.5) but, compared to the senescence/green-down phenophase, with increasing net radiation and air temperature (Fig. 3). Compared to the maturity/peak and the senescence\green-down phenophases, the dormant and green-up phenophases showed relatively higher variations and lower correlation among satellite products estimates. The significant differences in satellite-based evaporation estimates during the dormant and green-up phenophases suggests that it is more challenging to estimate Miombo evaporation in low moisture, low forest canopy cover and high available energy conditions. The green-up phenophase has relatively high canopy cover, rising soil moisture and high available

energy conditions that are similar to the maturity/peak and senescence phenophases. The discrepancies observed during the green-up phenophase may be more related to the ability of the satellite-based estimates to effectively account for rainfall interception at the commencement of the rain season.
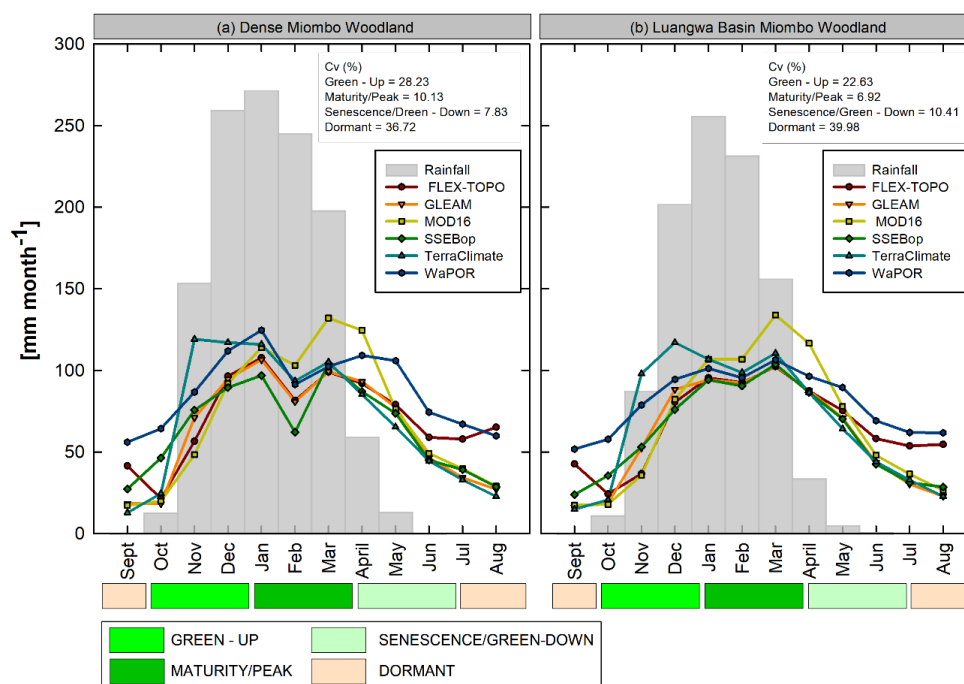
Figure 5. Comparison of aggregated (2009-2020) mean estimates of actual evaporation by satellite products across hydrological year (September – August) in the Luangwa Basin.

3.2.3 Variations in climate and phenological variables reflected in satellite-based evaporation estimates

Figure 6 and Table A2 in the appendices shows across estimates and within estimates variation in each phenophase. The standard deviation (SD) is used to show the within estimates variations while the coefficient of variation (C_V) is used for inter estimates comparison. The senescence/green-down phenophases showed the lowest differences (7.83 %) among the satellite-based evaporation estimates, and was followed by maturity/peak phenophase ($C_V = 10.13$ %). The highest difference was in the dormant phenophase (36.72 %) while the green – up phenophase showed 28.33 percent variation. The least within estimates variations, with SD range of 5.72 – 10.04 mm month^{-1} was observed in the dormant phenophase, and was followed by the maturity/peak phenophase with SD range of 7.61 – 14.55 mm month^{-1}. The highest within estimates variation was observed in the green-up phenophase (19.12 – 46.81 mm month^{-1}). This was followed by the senescence/green-down phenophase with SD range of 14.34 – 29.0 mm month^{-1}. Some products (i.e., FLEX-TOPO and TerraClimate) showed relatively higher within estimates variation in the dormant phenophase compared to the maturity/peak phenophase while the other estimates showed higher variations in the maturity phenophase compared to the dormant

phenophase. The within satellite-based evaporation estimates variations (Fig. 6 a, b and Table A2 in the appendices) may be attributed to variations in climate and phenological variables that included rainfall, temperature, soil moisture and changes in canopy cover and chlorophyll (i.e., NDVI and LAI) in each phenophase. The within satellite-based climate and phenological variables variations were reflected in the within variations in satellite-based actual evaporation estimates (Fig. 6 b, c). For instance, lower within satellite-based actual evaporation estimates variations were observed during the dormant phenophase (period of no rainfall, low soil moisture, low canopy

600 cover, and low chlorophyll) and the maturity/peak phenophase (period of stable rains and consistently high canopy cover and chlorophyll) (Fig. 6 b). These two phenophases had the least variations in rainfall, air temperature and LAI/NDVI (Fig. 6 c).
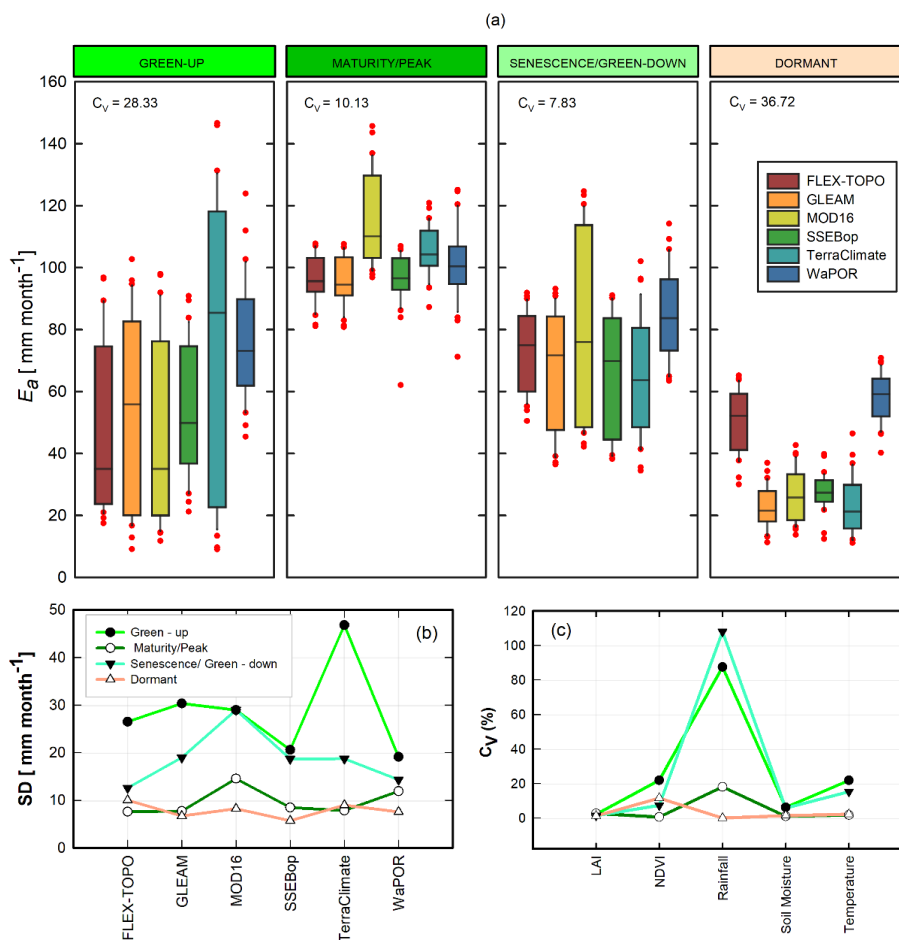
Figure 6. (a) Comparison of satellite data-based evaporation estimates across phenophases based on hydrological year at the dense Miombo Woodland scale. Most variations in actual evaporation estimates were observed in the dormant and green up phenophases. (b) Standard deviations and coefficients of variation for satellite-based evaporation estimates and climate and phenological variables across phenophases in the Miombo Woodland, Luangwa Basin.

Increased variations in NDVI during the dormant (Fig. 6 c) and green-up phenophases may be attributed to the changes in forest canopy leaf colour. The dormant phenophase is the driest part of the year with lowest canopy cover and chlorophyll. Significant within satellite-based estimates variations were observed at the boundaries, rain season to dry season, and the dry season to rain season, during the senescence/green-down and the green-up phenophases. This behaviour may be explained by the significant variations in precipitation during these two phenophases (Fig. 6 c).

640 ### 3.2.4 Spatial variations in satellite-based evaporation estimates

Figure 7 shows spatial distribution of satellite-based actual evaporation estimates across phenophases. The comparison was based on the entire Luangwa Basin, including non-Miombo regions. During the dormant phenophase, all six estimates appeared to show higher actual evaporation in forested upland Miombo areas than in other land cover types (Fig. 7) (refer to Fig. 2 and Fig. A1 in the appendices for extent of Miombo Woodland cover in the Luangwa Basin). Among many contributing factors, the land cover product as a model input in satellite-based evaporation estimates may largely explain the observed discrepancies in the spatial distribution of evaporation.
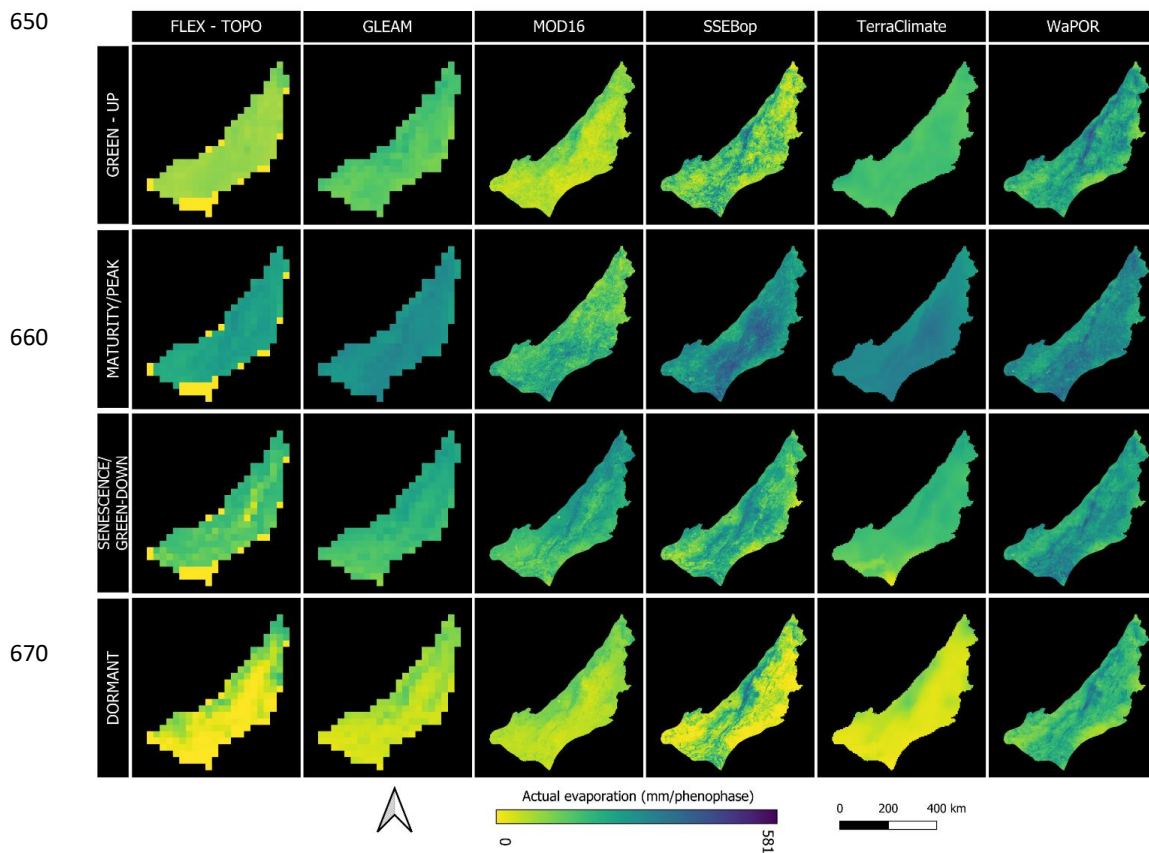

Figure 7. Spatial evaporation distribution of satellite-based evaporation estimates (per phenophase) across phenophases in the Luangwa basin.

Hydrology and
Earth System
Sciences
Discussions
Open Access

EGU

For instance, the MOD16 heavily relies on a global land-cover product (Gray *et al*., 2019; Running *et al*., 2019) which had shown to misclassify certain land cover types and showed low user
680   accuracy in certain regions (i.e., Leroux *et al.,* 2014).

      The WaPOR uses the Copernicus land cover product, but adds the distinction between irrigated and rain-fed areas (FAO, 2018). For the vegetation fraction, the GLEAM uses the MODIS MOD44B product (Martens *et al.,* 2017; Miralles *et al.,* 2011). Different vegetation types have different phenology and physiological attributes (i.e., Lu *et al*., 2006) which influences how actual evaporation is estimated. Miombo Woodland's dry season evaporation mainly occurs through plant transpiration, which is dependent on the landcover type, and is driven by root zone water availability and climate variables such as net radiation, air pressure, wind speed, air temperature and relative humidity. The link between the drivers and the plant transpiration is the stomata conductance thresholds which are vegetation type dependent (ie., Urban *et al.,* 2017; Wehr *et al.,*
690   2017; Tuzet, 2011). Therefore, dissimilarities in the land cover products and their associated accuracy limitations possibly reflect in differences in the spatial distribution of the satellite-based actual evaporation estimates.

### 3.3   Heterogeneity in forest canopy cover across phenophases

      Figure 8 shows the heterogeneity in tree canopy leaf fall among Miombo species during the dormant phenophase. Figure 9 shows the heterogeneity in forest canopy conditions across phenophases. The temporal changes in the satellite-based LAI and NDVI appeared to align well with the observed changes in forest canopy cover characteristics at the Mpika Miombo forest site. Lowest LAI and NDVI values were observed during the dormant phenophase. This is the period
700   with increased leaf fall, leaf flush and leaf colour changes as shown by the photographs in Fig. 8 and Fig. 9. It was observed that woody vegetation species like the Miombo could start growth using stored carbon reserves acquired during the previous season (Higgins and Scheiter, 2012). In the Miombo Woodland soil moisture increases with soil depth and remains relatively high in deep soils beyond 30 cm depth but varies with season (i.e., Chidumayo, 1994). Miombo species are said to have developed mechanisms such as extensive lateral and deep rooting (of up to 25 m in some species), creating capacity for access to ground water resources in deep soils; the plants also shed off leaves and utilise stem water storage as part of the system to buffer water limited conditions in the dry season (Vinya *et al.,* 2018; Tian *et al.,* 2018; Guan *et al.*, 2014). However, there is also early flushing before the commencement of seasonal rainfall (Chidumayo, 1994; Fuller and Prince,
710   1996). While at individual species level the entire tree canopy can be leaf less (i.e., Fig. 8), or changing leaf colour, this is not the same at forest canopy level due to heterogeneity in species phenological changes (i.e., Figs. 8 & 9).

      During the transition period high variability is observed in the leaf fall and leaf flush among Miombo species (i.e., Zimba *et al.,* 2020; Vinya *et al.,* 2018, Fuller, 1999; Frost, 1996 and Figs. 8 & 9). This implies that while some species are transpiring others are in dormant stage. Therefore, with access to groundwater and vegetative water storage the field actual evaporation in the dormant and green-up phenophase is likely to be higher than satellite-based estimates as demonstrated by Zimba *et al.* (2022).
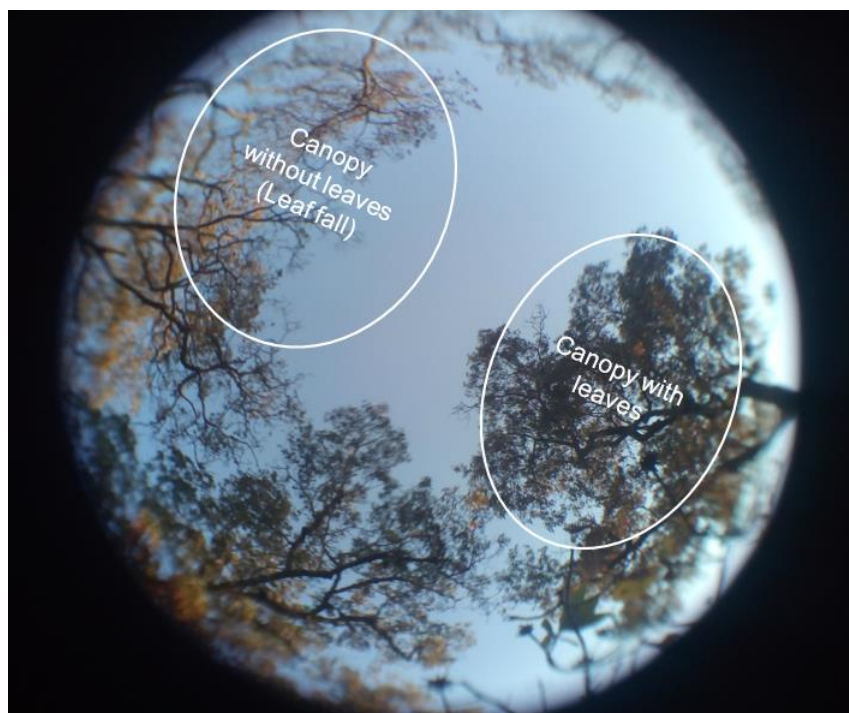
720   .

Figure 8. Heterogeneity in leaf fall and leaf flush activities among Miombo species at the Mpika Miombo Woodland site. Photograph taken on 10th, September, 2021.

750   At forest canopy level, these dormant and green-up phenophase Miombo species adapted characteristics influence the dry season Miombo Woodland transpiration and rainfall interception at the onset of the rain season. It follows then that if the structure, processes and inputs of the models, from which satellite-based actual evaporation estimates are derived, do not have capacity to capture these dry season Miombo Woodland phenological attributes, this potentially influences estimates of transpiration in the dry season and rainfall interception at the commencement of the rain season. For instance, if dormant phenophase transpiration is not coupled with the vertical upward moisture interaction such as access to ground water, as is the case with GLEAM, there exists high potential by satellite-based evaporation estimates to have an incorrect trend and magnitude of actual evaporation.

760   Maturity and peak phenophases showed the least differences in actual evaporation estimates across satellite-based evaporation estimates. This means that the satellite-based evaporation estimates had similar behaviour during periods of high forest canopy cover, high atmospheric and soil moisture, and high chlorophyll levels. This scenario appeared to hold even under the senescence and green-down phenophases.

     It appeared that the changing conditions in plant phenology and its interaction with climate and hydrological variables in the dormant and green-up phenophases may be what brings about the large differences in the behaviour of the dry season satellite-based actual evaporation estimates. Possible contributing factors to the behaviour of satellite-based evaporation estimates across phenophases have been highlighted in Zimba *et al.* (2022).
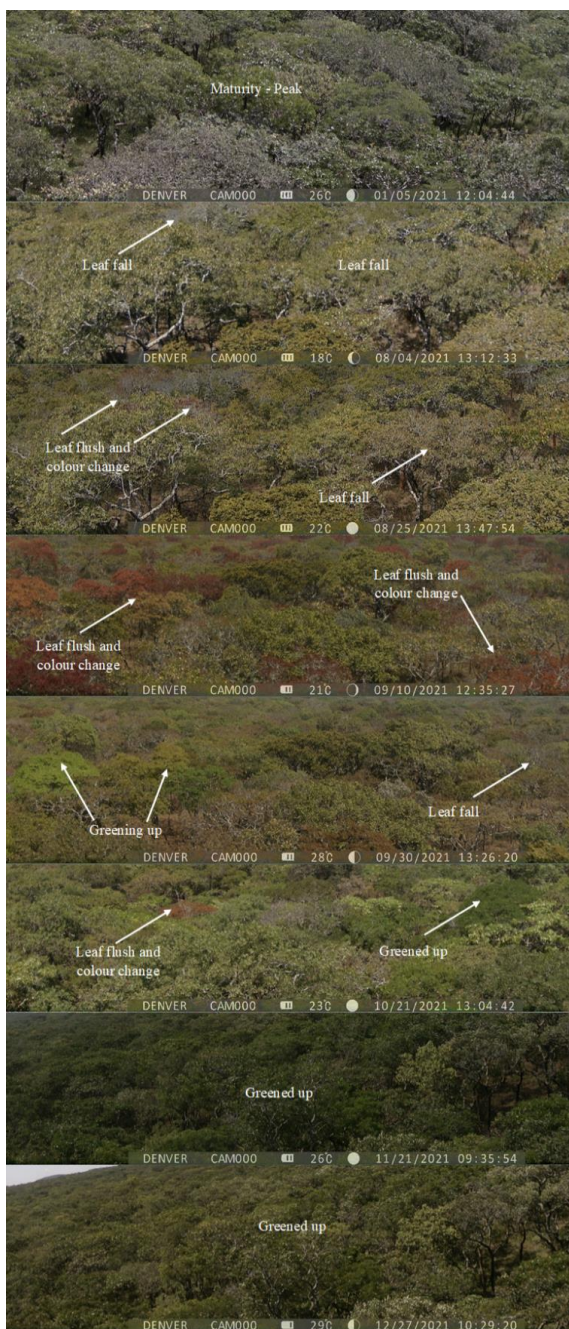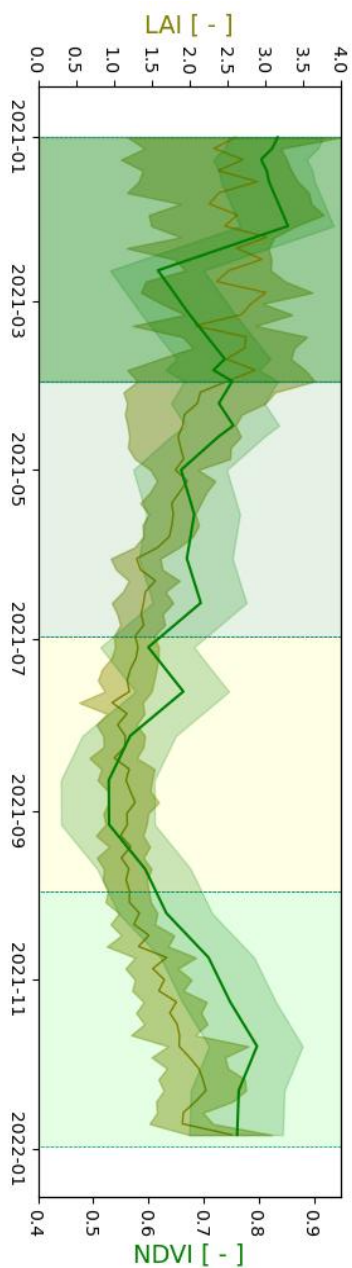
770

780

790

800

810

Figure 9. Temporal behaviour of MODIS LAI, NDVI, and the Miombo Forest canopy display behaviour for the year 2021 at Mpika station. Shaded area are phenophases: January – March is the Maturity/Peak; April-June is the Senescence/Green-down; July-September is the Dormant while October – December is the green-up. Shaded area for variables is the standard deviation

18

3.4 Comparison of satellite-based actual evaporation estimates with the water balance-based evaporation estimates

Figures 10 shows the results of the temporal comparison of satellite-based actual evaporation estimates with the water balance estimates at Luangwa Basin scale. This comparison included non-Miombo areas as the runoff estimates, used to calibrate the FLEX-Topo, were for the entire Luangwa Basin, including non-Miombo areas. All satellite-based evaporation estimates showed insignificant correlation ($p\text{-}value > 0.05$) with the water balance evaporation (E_{wb}) (Table A3 in the appendices). Compared with the E_{wb} estimates, all six satellite-based evaporation estimates underestimated actual evaporation (Fig. 10). In any given year, the WaPOR appeared to have the least underestimation with an aggregated mean bias of 120 mm year^{-1}, while the GLEAM had the largest underestimation with an aggregated mean bias of 370 mm year^{-1}. Only the SSEBop and the WaPOR showed a below average aggregated annual mean bias (in dotted red line) (Fig. 10 c).

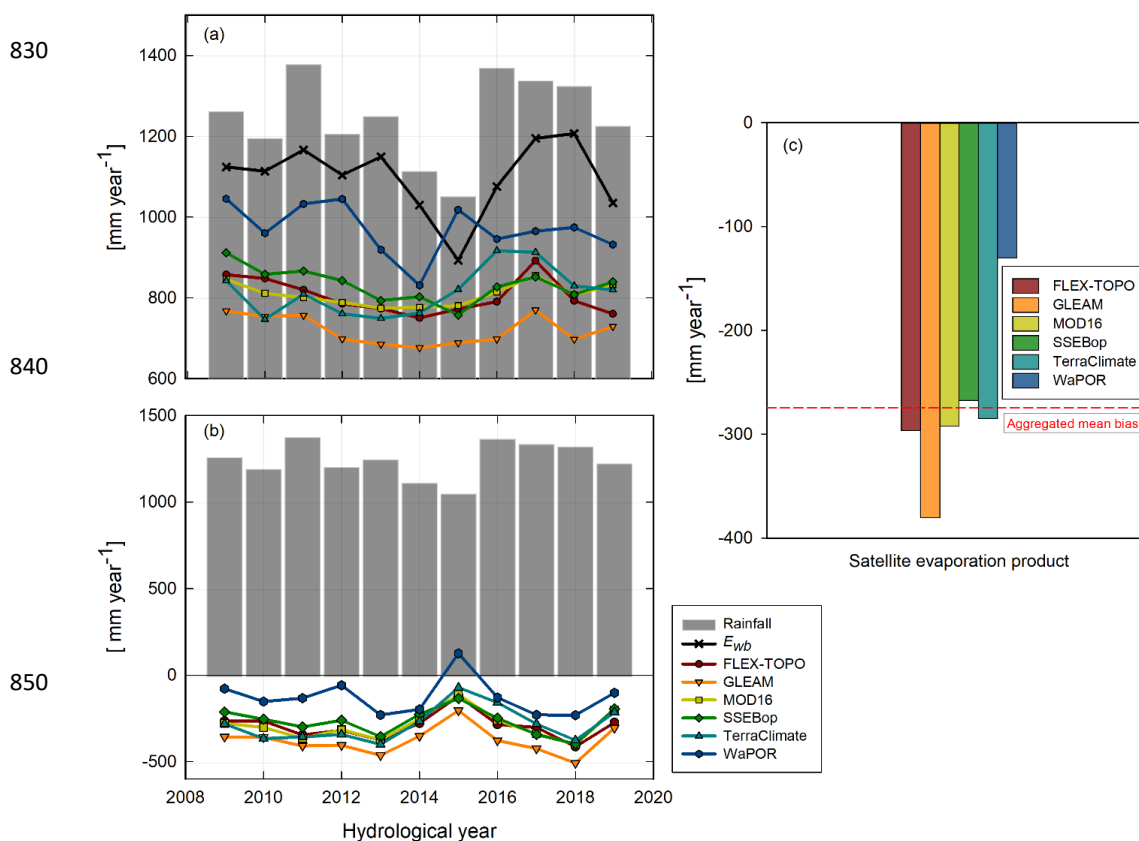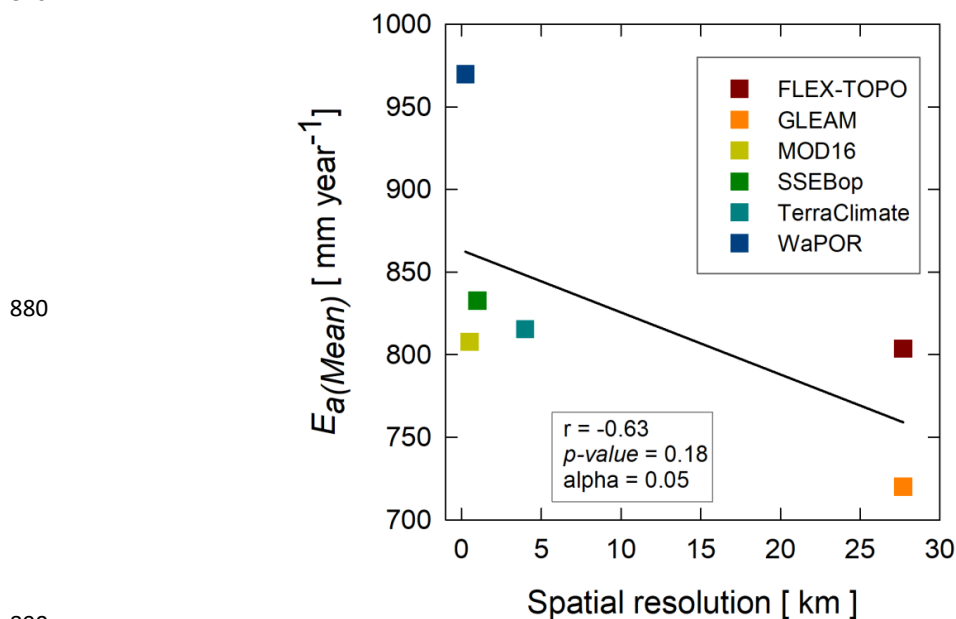*Figure 10. (a) Comparison of satellite-based evaporation estimates and the water balance-based estimates of actual evaporation for Luangwa Basin and (b, c) the results of the bias assessment.*

At basin scale, it appeared there was no statistically significant correlation ($r = -0.63$; $p\text{-}value = 0.18$; alpha = 0.05) between spatial resolution of satellite-based evaporation estimates and

evaporation estimates of each product (Fig. 11). For instance, the TerraClimate, with a relatively coarser spatial resolution, compared to finer spatial resolution products MOD16 and SSEBop, showed relatively similar bias estimates. The MOD16 had a higher resolution than the SSEBop, but underestimated more. The FLEX-Topo had a coarser resolution than the MOD16 and the SSEBop but exhibited higher estimates in the dormant phenophases (July-September) (Fig. 5). The lack of a clear significant relationship, between spatial resolution and actual evaporation estimates (Fig. 11) may imply that, other factors such as the heterogeneity in the land cover, differences in model structure, processes and model inputs may be the largest contributing factors of the observed discrepancies in the actual evaporation estimates at basin scale.

870

Figure 11. Basin scale correlation of actual evaporation estimates with spatial resolution of satellite-based evaporation estimates

The water balance assessment included non-Miombo woodlands. However, about 75 percent of the Luangwa Basin comprises Miombo Woodland. The assumption was that the observed underestimation of satellite estimates, in comparison to E_{wb}, was largely affected by difficulty to assess Miombo Woodland actual evaporation, especially in the dormant and green-up phenophases. The results of the comparison of the water balance-based evaporation estimates with satellite-based evaporation estimates agreed with the point-based field actual evaporation estimates by Zimba *et al.* (2022) which that showed satellite-based evaporation estimates underestimated actual evaporation during the dormant and green-up phenophases at a Miombo Woodland site in Mpika in the Luangwa Basin. The results of this study also agreed with Weerasinghe *et al.* (2020) who showed that most evaporation products generally underestimated evaporation across African basins though SSEBop and WaPOR showed mixed behaviour of both underestimating and overestimating. In this study, in comparison to other satellite-based evaporation estimates, the SSEBop and WaPOR appeared to have lower underestimations. This

behaviour (i.e., trend and magnitude) of the SSEBop and the WaPOR agreed with the point scale field observations (Zimba *et al.*, 2022) and suggests the two estimates could be close to field actual evaporation of the Miombo Woodland in the Luangwa Basin and Miombo region in general.

910

4   Conclusions and recommendations

This study aimed at comparing phenophase-based actual evaporation estimates of different satellite-based evaporation estimates in the largely Miombo covered woodland of the Luangwa Basin. The study sought to find out the extent to which satellite-based estimates of evaporation were similar across Miombo phenophases. We observed the phenophases in which satellite-based evaporation estimates differ, and showed the potentially underlying factor(s) for the discrepancies. Furthermore, the study compared the satellite-based actual evaporation estimates to the general water balance-based evaporation at basin scale. This helped establish which of the satellite-based evaporation estimates were close to the field conditions in the Luangwa Basin. We arrived at the following conclusions:

920

(i)   Satellite-based evaporation estimates appeared to have difficulty estimating evaporation in the dormant and green-up phenophases. This was evidenced by the large discrepancies (i.e., coefficients of variations) in satellite-based evaporation estimates observed during these phenophases. The limited understanding and lack of representation in models of the typical traits of The Miombo Woodland phenology interaction with climate and access to deep soil moisture stocks (and possibly to ground water) during these phenophases is not well understood and lacks representation in models. This is what could have contributed to the relatively poor performance of satellite-based evaporation estimates.

930

(ii)   Dry season wet Miombo forest canopy cover, proxied by the Mpika study site, remained relatively high, green and healthy ($LAI \approx 0.6$; $NDVI \approx 0.5$) with capacity for continued transpiration. This may have been aided by the physiologically adapted access to deep soil moisture and vegetation water storage. Therefore, satellite-based evaporation estimates that are better equipped to account for the Miombo Woodland physiological interaction with climate variables during the dormant phenophase are likely to provide better evaporation estimates.

940

(iii)   Satellite-based evaporation estimates show similar behaviours during the maturity, peak, senescence and green-down phenophases in the rain season, as evidenced by the small variation (i.e., coefficients of estimates) in evaporation estimates. During these phenophases the forest canopy cover, available energy, water availability and vegetation photosynthetic activities were high. Consequently, this may mean that a large portion of the observed underestimation, with reference to the water balance evaporation at annual scale, may be accounted for by the challenges in estimating dormant and green-up phenophases evaporation.

950

(iv)   At basin scale, the spatial resolution of satellite-based evaporation estimates appeared to be statistically insignificant in estimating evaporation. With an exception of the WaPOR, which had the finest spatial resolution, FLEX-Topo, MOD16, SSEBop and TerraClimate estimates were relatively similar despite

having varying spatial resolutions. For example, in the senescence/green-down and dormant phenophases, FLEX-Topo, a product with a coarser resolution showed higher estimates of evaporation compared to products with relatively finer resolutions like MOD16, SSEBop and TerraClimate. Overall, SSEBop, with a coarser resolution, relative to MOD16 showed lower underestimation. These observations suggested that, among other factors, the model structure, processes and inputs may influence satellite evaporation estimates in the Miombo Woodland.

960

(v)   With reference to the water balance evaporation, WaPOR appeared to underestimate the least and is likely to be close to field conditions. This is possibly facilitated by the WaPOR model structure, inputs and processes such as the Copernicus land cover product and the energy partitioning.

(vi)   Overall, plant phenology appeared to influence dry season satellite-based evaporation estimates. Therefore, understanding the Miombo Woodland phenology interaction with water and climate variables, and accounting for these in the model structure, processes and inputs, is likely to improve satellite-based evaporation estimates in this complex ecosystem.

970

(vii)   Consequently, field observations across phenophases, of Miombo Woodland evaporation are needed in order to establish the correct actual evaporation characteristics. This will help improve satellite-based evaporation assessments in the Luangwa Basin and the Miombo region as whole.

Code availability
Code for FLEX-Topo model can be requested from the authors

980 **Author contributions**
Conceptualization, H.M.Z, H.H.G.S.; formal analysis, H.Z.; resources, H.H.G.S. and N.G; supervision, M.C.-G. and B.K.; writing—original draft, H.Z.; writing—review and editing, M.C.-G., B.K., H.S., N.G, P.H and H.H.G.S. FLEX-Topo model set up and simulations, P.H. All authors have read and agree to the published version of the manuscript.

Competing interests
At least one of the (co-)authors is a member of the editorial board of Hydrology and Earth System Sciences.
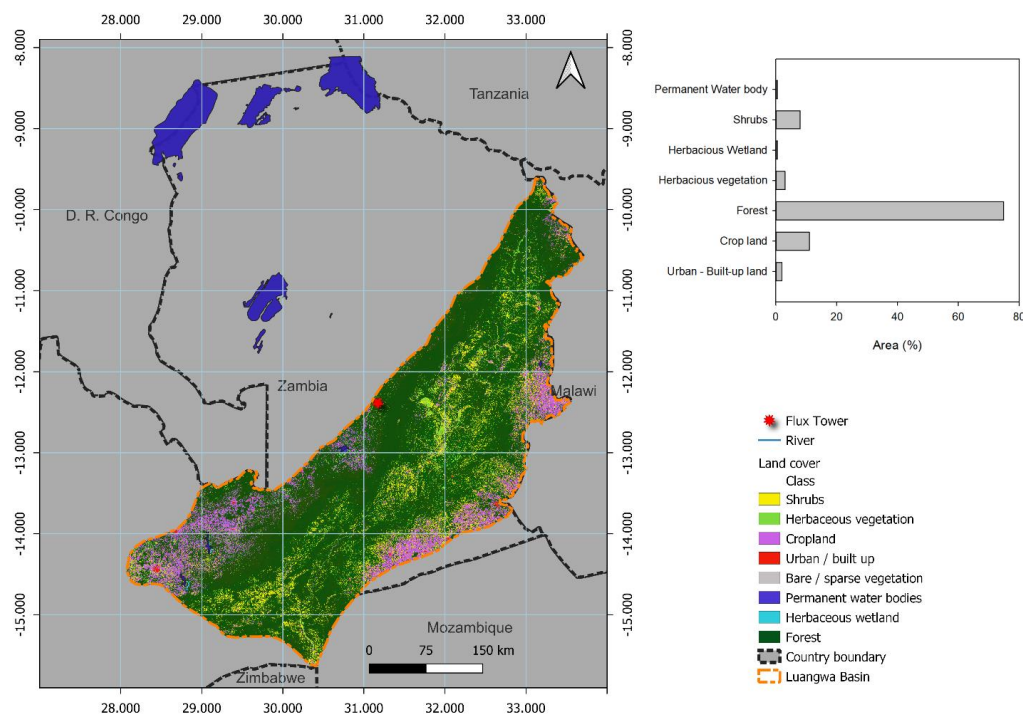
Appendices

1000

Figure A1. 2019 Copernicus land cover classification of the Luangwa Basin

Table A1. Kendall correlation coefficients of satellite-based evaporation estimates   across Miombo woodland phenophases in the Luangwa Basin

	PHENOPHASE									
	GREEN UP					**MATURITY-PEAK**				
Product	GLEAM	MOD16	SSEBop	TerraClimate	WaPOR	GLEAM	MOD16	SSEBop	TerraClimate	WaPOR
FLEX-Topo	**0.81**	0.09	0.22	-0.17	-0.11	**0.89**	0.08	0.14	0.19	-0.04
GLEAM	**1.00**	0.07	0.21	-0.20	-0.16	**1.00**	0.05	0.15	0.17	-0.05
MOD16		**1.00**	0.11	**0.40**	0.02		**1.00**	0.43	0.53	0.17
SSEBop			**1.00**	-0.09	0.09			**1.00**	0.31	0.20
TerraClimate				**1.00**	0.09				**1.00**	0.20
WaPOR					**1.00**					**1.00**

	SENESCENCE -GREEN DOWN					DORMANT				
Product	GLEAM	MOD16	SSEBop	TerraClimate	WaPOR	GLEAM	MOD16	SSEBop	TerraClimate	WaPOR
FLEX-Topo	**0.92**	0.14	0.05	0.11	0.04	**0.54**	-0.05	-0.13	**-0.25**	0.20
GLEAM	**1.00**	0.11	0.02	0.09	0.01	**1.00**	-0.06	-0.17	-0.19	0.16
MOD16		**1.00**	0.36	**0.64**	0.19		**1.00**	-0.05	**0.38**	0.00
SSEBop			**1.00**	0.42	0.23			**1.00**	-0.17	-0.09
TerraClimate				**1.00**	0.12				**1.00**	**-0.31**
WaPOR					**1.00**					**1.00**

Hydrology and
Earth System
Sciences
Discussions

Table A2. Satellite product phenophase mean, standard deviation and coefficients of variation (%) for the Miombo Woodland

Product	Green up			MATURITY/PEAK			SENESCENCE/GREEN-DOWN			DORMANT		
	μ	σ	C_V	μ	σ	C_V	μ	σ	C_V	μ	σ	C_V
FLEX-TOPO	47.18	26.52	55.36	96.76	7.61	7.75	73.65	12.59	16.84	50.34	10.04	19.64
GLEAM	53.18	30.34	56.19	96.39	7.74	7.91	67.33	18.99	27.78	23.12	6.72	28.64
MOD16	45.37	28.97	62.87	115.93	14.55	12.36	80.84	29.00	35.32	26.81	8.24	30.28
SSEBop	54.89	20.61	36.97	96.14	8.50	8.70	66.40	18.72	27.77	27.92	5.72	20.18
TerraClimate	78.57	46.81	58.67	105.36	7.86	7.34	64.91	18.74	28.43	23.53	8.99	37.62
WaPOR	77.02	19.12	24.45	101.10	11.91	11.60	85.00	14.34	16.61	58.49	7.58	12.77

μ = mean, σ = standard deviation, C_V = coefficient of variation

Table A3. Kendall Correlation coefficient of satellite-based evaporation estimates, rainfall and the water balance evaporation in the Luangwa Basin

Product	Rainfall	E_{wb}	FLEX-TOPO	GLEAM	MOD16	SSEBop	TerraClimate	WaPOR
Rainfall	**1.00**	**0.79**	0.45	0.44	0.49	0.50	0.54	0.20
E_{wb}		**1.00**	0.55	0.44	0.38	0.51	0.12	0.11
FLEX-TOPO			**1.00**	**0.87**	**0.73**	**0.68**	0.41	0.42
GLEAM				**1.00**	**0.80**	**0.83**	0.31	0.43
MOD16					**1.00**	**0.70**	**0.67**	0.24
SSEBop						**1.00**	0.18	0.40
TerraClimate							**1.00**	0.16
WaPOR								**1.00**

Values in bold are different from 0 with a significance level alpha=0.05

References

Abatzoglou, J. T., Dobrowski, S. Z., Parks, S. A., & Hegewisch, K. C.,: TerraClimate, a high-resolution global dataset of monthly climate and climatic water balance from 1958-2015. *Scientific Data*, 5, 1–12. doi:10.1038/sdata.2017.191, 2018.

Abrams, M., & Crippen, R.,: ASTER Global DEM (Digital Elevation Mode) - Quick Guide for V3. *California Institute of Technology*, 3(July), 10., 2019.

Asadullah, A., McIntyre, N., & Kigobe, M.: Evaluation of five satellite products for estimation of rainfall over Uganda. *Hydrological Sciences Journal*, 53(6), 1137–1150. doi: 10.1623/hysj.53.6.1137, 2008.

Beilfuss, R.: *A Risky Climate for Southern African Hydro ASSESSING HYDROLOGICAL RISKS AND A Risky Climate for Southern African Hydro*. *September*. doi: 10.13140/RG.2.2.30193.48486, 2012.

Bonnesoeur, V., Locatelli, B., Guariguata, M. R., Ochoa-Tocachi, B. F., Vanacker, V., Mao, Z., Stokes, A., & Mathez-Stiefel, S. L.: Impacts of forests and forestation on hydrological services in the Andes: A systematic review. *Forest Ecology and Management*, 433(June 2018), 569–584. doi: 10.1016/j.foreco.2018.11.033, 2019.

Buchhorn, M.; Smets, B.; Bertels, L.; De Roo, B.; Lesiv, M.; Tsendbazar, N.E., Linlin, L., Tarko, A.: *Copernicus Global Land Service: Land Cover 100m: Version 3 Globe 2015-2019: Product User Manual*. Zenodo, Geneve, Switzerland. doi: 10.5281/zenodo.3938963, 2020.

Chidumayo, E. N.,: Climate and Phenology of Savanna Vegetation in Southern Africa. *Journal of Vegetation Science*, *12*(3), 347. doi: 10.2307/3236848, 2001.

Chidumayo, E. N.: Phenology and nutrition of miombo woodland trees in Zambia. *Trees*, *9*(2), 67–72. doi: 10.1007/BF00202124, 1994.

1070   Cleland, E. E., Chuine, I., Menzel, A., Mooney, H. A., & Schwartz, M. D.: Shifting plant phenology in response to global change. *Behaviours in Ecology and Evolution*, *22*(7), 357–365. doi: 10.1016/j.tree.2007.04.003, 2007.

Didan, K., Munoz, A. B., Solano, R., & Huete, A.: *MODISVegetationIndexUser'sGuide(MOD13Series).* Arizona: The Universoty of Arizon, 2015.

Dinku, T., Ceccato, P., Grover-Kopec, E., Lemma, M., Connor, S. J., & Ropelewski, C. F.: Validation of satellite rainfall products over East Africa's complex topography. *International Journal of Remote Sensing*, *28*(7), 1503–1526. doi: 10.1080/01431160600954688, 2007.

1080   FAO.: WaPOR Database Methodology: Level 1 Data. In Remote Sensing for Water Productivity Technical Report: Methodology Series. (Issue September). Retrieved from http://www.fao.org/fileadmin/user_upload/faoweb/RS-WP/pdf_files/Web_WaPOR-beta_Methodology_document_Level1.pdf, 2018.

Forrest, J., Inouye, D. W., & Thomson, J. D.: Flowering phenology in subalpine meadows: Does climate variation influence community co-flowering behaviours? *Ecology*, *91*(2), 431–440. doi: 10.1890/09-0099.1, 2010.

Forrest, J., & Miller-Rushing, A. J.: Toward a synthetic understanding of the role of phenology in ecology and evolution. *Philosophical Transactions of the Royal Society B: Biological Sciences*, *365*(1555), 3101–3112. doi: 10.1098/rstb.2010.0145, 2010.

1090   Forster, M. A., Kim, T. D. H., Kunz, S., Abuseif, M., Chulliparambil, V. R., Srichandra, J., & Michael, R. N.: Phenology and canopy conductance limit the accuracy of 20 evapotranspiration models in predicting transpiration. *Agricultural and Forest Meteorology*, *315*(December 2021), 108824. doi: 10.1016/j.agrformet.2022.108824, 2022.

Frost, P.: The Ecology of Miombo Woodlands. In The Miombo in Transition: Woodlands and Welfare in Africa. Retrieved from http://books.google.com/books?hl=nl&lr=&id=rpildJJVdU4C&pgis=1, 1996.

Fuller, D. O.: Canopy phenology of some mopane and miombo woodlands in eastern Zambia. *Global Ecology and Biogeography*, *8*(3–4), 199–209. doi: 10.1046/j.1365-2699.1999.00130.x, 1999.

1100   Fuller, D. O., & Prince, S. D.: Rainfall and foliar dynamics in tropical southern Africa: Potential impacts of global climatic change on Savanna vegetation. *Climatic Change*, *33*(1), 69–96. doi: 10.1007/BF00140514, 1996.

Funk, C., Peterson, P., Landsfeld, M., Pedreros, D., Verdin, J., Shukla, S., … Michaelsen, J.: The climate hazards infrared precipitation with stations - A new environmental record for

monitoring extremes. *Scientific Data*, *2*, 1–21. doi:10.1038/sdata.2015.66, 2015.

García, L., Rodríguez, J. D., Wijnen, M., & Pakulski, I.: *Earth Observation for Water Resources Management: Current Use and Future Opportunities for the Water Sector*. Washington, DC 20433: Washington, DC: World Bank. doi: 10.1596/978-1-4648-0475-5, 2016.

Gerrits, A. M.,: *The role of interception in the hydrological cycle.* Delft, the Netherlands: VSSD. Retrieved from http://www.interception.citg.tudelft.nl/, 2010.

Gray, J., Sulla-Menashe, D., & Friedl, M. A.: MODIS Land Cover Dynamics (MCD12Q2) Product. *User Guide Collection 6*, *6*, 8. Retrieved from https://modis-land.gsfc.nasa.gov/pdf/MCD12Q2_Collection6_UserGuide.pdf, 2019.

Guan, K., Wood, E. F., Medvigy, D., Kimball, J., Pan, M., Caylor, K. K., Sheffield, J., Xu, X., & Jones, O. M.: *phenology of African savannas and woodlands*. *119*, 1652–1669. doi: 10.1002/2013JG002572, 2014.

Helsel, D. R., R. M. Hirsch, K.R. Ryberg, S.A. Archfield, and E.J. Gilroy..: "Statistical Methods in Water Resources Techniques and Methods 4 – A3." *USGS Techniques and Methods*, 2020.

Hersbach, H., Bell, B., Berrisford, P., Hirahara, S., Horányi, A., Muñoz-Sabater, J., Nicolas, J., Peubey, C., Radu, R., Schepers, D., Simmons, A., Soci, C., Abdalla, S., Abellan, X., Balsamo, G., Bechtold, P., Biavati, G., Bidlot, J., Bonavita, M., De Chiara, G., Dahlgren, P., Dee, D., Diamantakis, M., Dragani, R., Flemming, J., Forbes, R., Fuentes, M., Geer, A., Haimberger, L., Healy, S., Hogan, R.J., Hólm, E., Janisková, M., Keeley, S., Laloyaux, P., Lopez, P., Lupu, C., Radnoti, G., de Rosnay, P., Rozum, I., Vamborg, F., Villaume, S., Thépaut, J-N.: Complete ERA5 from 1979: Fifth generation of ECMWF atmospheric reanalyses of the global climate. Copernicus Climate Change Service (C3S) Data Store (CDS). (Accessed on 10-01-2021), 2017.

Higgins, S. I., & Scheiter, S.: Atmospheric CO $_2$ forces abrupt vegetation shifts locally, but not globally. *Nature*, *488*(7410), 209–212. doi: 10.1038/nature11238, 2012.

Hulsman, P., Hrachowitz, M., & Savenije, H. H. G.: Improving the Representation of Long-Term Storage Variations With Conceptual Hydrological Models in Data-Scarce Regions. *Water Resources Research*, *57*(4). doi: 10.1029/2020WR028837, 2021.

Hulsman, P., Winsemius, H. C., Michailovsky, C. I., Savenije, H. H. G., & Hrachowitz, M.: Using altimetry observations combined with GRACE to select parameter sets of a hydrological model in a data-scarce region. *Hydrology and Earth System Sciences*, *24*(6), 3331–3359. doi: 10.5194/hess-24-3331-2020, 2020.

Kleine, L., Tetzlaff, D., Smith, A., Dubbert, M., & Soulsby, C.: Modelling ecohydrological feedbacks in forest and grassland plots under a prolonged drought anomaly in Central Europe 2018–2020. *Hydrological Processes*, *35*(8). doi: 10.1002/hyp.14325, 2021.

Kramer, K., Leinonen, I., & Loustau, D.: The importance of phenology for the evaluation of impact of climate change on growth of boreal, temperate and Mediterranean forests ecosystems: An overview. In International Journal of Biometeorology (Vol. 44, Issue 2, pp.

Hydrology and
Earth System
Sciences
Discussions

Open Access
EGU

67–75). doi: 10.1007/s004840000066, 2000.

Leroux, L., Jolivot,A., Bégué,A., Lo Seen,D., and Zoungrana, B.,: "How Reliable Is the MODIS Land Cover Product for Crop Mapping Sub-Saharan Agricultural Landscapes?" *Remote Sensing* 6(9):8541–64. doi: 10.3390/rs6098541, 2014.

1150 Liu, W., Wang, L., Zhou, J., Li, Y., Sun, F., Fu, G., Li, X., & Sang, Y. F.: A worldwide evaluation of basin-scale evapotranspiration estimates against the water balance method. *Journal of Hydrology*, *538*, 82–95. doi: 10.1016/j.jhydrol.2016.04.006, 2016.

Lu, P., Yu, Q., Liu, J., & Lee, X.: Advance of tree-flowering dates in response to urban climate change. *Agricultural and Forest Meteorology*, *138*(1–4), 120–131. doi: 10.1016/j.agrformet.2006.04.002, 2006.

Macharia, D., Fankhauser, K., Selker, J. S., Neff, J. C., & Thomas, E. A.: Validation and Intercomparison of Satellite-Based Rainfall Products over Africa with TAHMO In Situ Rainfall Observations. *Journal of Hydrometeorology*, *23*(7), 1131–1154. doi: 10.1175/JHM-D-21-0161.1, 2022.

1160 Makapela, L.: *Review and use of earth observations and remote sensing in water resource management in South Africa : report to the Water Research Commission* (Issue October 2015), 2015.

Marchesini, V. A., Fernández, R. J., Reynolds, J. F., Sobrino, J. A., & Di Bella, C. M.: Changes in evapotranspiration and phenology as consequences of shrub removal in dry forests of central Argentina. *Ecohydrology*, *8*(7), 1304–1311. doi: 10.1002/eco.1583, 2015.

Martens, B., Miralles, D. G., Lievens, H., Van Der Schalie, R., De Jeu, R. A. M., Fernández-Prieto, D., Beck, H. E., Dorigo, W. A., & Verhoest, N. E. C.: GLEAM v3: Satellite-based land evaporation and root-zone soil moisture. *Geoscientific Model Development*, *10*(5), 1903–1925. doi: 10.5194/gmd-10-1903-2017, 2017.

1170 Martins, J. P., Trigo, I., & Freitas, S. C. e.: Copernicus Global Land Operations "Vegetation and Energy" "CGLOPS-1". *Copernicus Global Land Operations*, 1–93. doi: 10.5281/zenodo.3938963.PU, 2020.

Miralles, D. G., Brutsaert, W., Dolman, A. J., & Gash, J. H.: On the Use of the Term "Evapotranspiration". *Water Resources Research*, *56*(11). doi: 10.1029/2020WR028055, 2020.

Miralles, D. G., De Jeu, R. A. M., Gash, J. H., Holmes, T. R. H., & Dolman, A. J.: Magnitude and variability of land evaporation and its components at the global scale. *Hydrology and Earth System Sciences*, *15*(3), 967–981. doi: 10.5194/hess-15-967-2011, 2011.

1180 Mu, Q., Zhao, M., and Running, W.S.,: "Improvements to a MODIS Global Terrestrial Evapotranspiration Algorithm." *Remote Sensing of Environment* 115 (8): 1781–1800. https://doi.org/10.1016/j.rse.2011.02.019, 2011.

Mu, Q., Heinsch, F. A., Zhao, M., & Running, S. W.: Development of a global evapotranspiration algorithm based on MODIS and global meteorology data. *Remote Sensing of Environment*, *111*(4), 519–536. doi: 10.1016/j.rse.2007.04.015, 2007.

Myneni, R., & Park, Y. K.: *MCD15A2H MODIS/Terra+Aqua Leaf Area Index/FPAR 8-day L4 Global 500m SIN Grid V006.* NASA EOSDIS Land Processes DAAC. Retrieved from https://doi.org/10.5067/MODIS/MCD15A2H.006, 2015.

1190   Niu,S., Fu,Y., Gu,L., and and Luo, Y.,: "Temperature Sensitivity of Canopy Photosynthesis Phenology in Northern Ecosystems." Pp. 503–19 in *Phenology: An Integrative Environmental Science*, edited by M. D. Schwartz., 2013

Nord, E. A., & Lynch, J. P.: Plant phenology: A critical controller of soil resource acquisition. *Journal of Experimental Botany*, *60*(7), 1927–1937. doi: 10.1093/jxb/erp018, 2009.

Pelletier, J., Paquette, A., Mbindo, K., Zimba, N., Siampale, A., Chendauka, B., Siangulube, F., & Roberts, J. W.: Carbon sink despite large deforestation in African tropical dry forests (miombo woodlands). *Environmental Research Letters*, *13*(9). doi: 10.1088/1748-9326/aadc9a, 2018.

Pereira, C. C., Boaventura, M. G., Cornelissen, T., Nunes, Y. R. F., & de Castro, G. C.: What triggers phenological events in plants under seasonal environments? A study with
1200   phylogenetically related plant species in sympatry. *Brazilian Journal of Biology*, *84*(March). doi: 10.1590/1519-6984.257969, 2022.

Roberts, J. M.: THE ROLE OF FORESTS IN THE HYDROLOGICAL CYCLE. In Forests and forest plants: Vol. III. Retrieved from https://www.eolss.net/sample-chapters/c10/E5-03-04-02.pdf, (undated).

Running, Steven W, Qiaozhen Mu, Maosheng Zhao, A. M.: *User ' s Guide MODIS Global Terrestrial Evapotranspiration (ET) Product NASA Earth Observing System MODIS Land Algorithm (For Collection 6)*, 2019.

Ryan, C. M., Pritchard, R., McNicol, I., Owen, M., Fisher, J. A., & Lehmann, C.: Ecosystem services from southern African woodlands and their future under global change.
1210   *Philosophical Transactions of the Royal Society B: Biological Sciences*, *371*(1703). doi: 10.1098/rstb.2015.0312, 2016.

Saha, , S., Moorthi, S., Wu, X., Wang, J., & Coauthors.,: The NCEP Climate Forecast System Version 2. *Journal of Climate, 27*, 2185–2208. doi:10.1175/JCLI-D-12-00823.1, 2014.

Saha, , S., Moorthi, S., Pan, H., Wu,, X., Wang, J., & Coauthors.,: The NCEP Climate Forecast System Reanalysis. *Bulletin of the American Meteorological Society, 91*, 1015–1057. doi:10.1175/2010BAMS3001.1, 2010.

Santin-Janin, H., Garel, M., Chapuis, J. L., & Pontier, D.: Assessing the performance of NDVI as a proxy for plant biomass using non-linear models: A case study on the kerguelen archipelago. *Polar Biology*, *32*(6), 861–871. doi: 10.1007/s00300-009-0586-5, 2009.

1220   Savenije, H. H.G.: HESS opinions 'topography driven conceptual modelling (FLEX-Topo)'. *Hydrology and Earth System Sciences*, *14*(12), 2681–2692. doi: 10.5194/hess-14-2681-2010, 2010.

Savenije, Hubert H.G.: The importance of interception and why we should delete the term evapotranspiration from our vocabulary. *Hydrological Processes*, *18*(8), 1507–1511. doi:

10.1002/hyp.5563, 2004.

Savoca, M. E., G. B. Senay, M. A. Maupin, J. F. Kenny, and C. A. Perry.,: "Actual
Evapotranspiration Modeling Using the Operational Simplified Surface Energy Balance (
SSEBop) Approach." *U.S Geologica Survey Scientific Investigations Report 2013–5126*,
no. January: 16 p. http://pubs.usgs.gov/sir/2013/5126, 2013.

1230

Schwartz, M. D.: Phenology: An Integrative Environmental Science. In M. D. Schwartz (Ed.),
Phenology: An Integrative Environmental Science (Second Edi). Dordrecht: Springer
Netherlands. doi: 10.1007/978-94-007-6925-0_27, 2013.

Shahidan, M. F., Salleh, E., & Mustafa, K. M. S.: Effects of tree canopies on solar radiation
filtration in a tropical microclimatic environment. *Sun, Wind and Architecture - The
Proceedings of the 24th International Conference on Passive and Low Energy Architecture,
PLEA 2007*, *November*, 400–406, 2007.

Sheil, D.: Forests, atmospheric water and an uncertain future: the new biology of the global
water cycle. *Forest Ecosystems*, *5*(1). doi: 10.1186/s40663-018-0138-y, 2018.

1240   Snyder, R. L., & Spano, D.: Phenology and Evapotranspiration. In Mark D. Schwartz (Ed.),
Phenology: An Integrative Environmental Science (Second, pp. 521–528). Milwaukee,
2013.

Stökli, R., Rutishauser, T., Baker, I., Liniger, M. A., & Denning, A. S.: A global reanalysis of
vegetation phenology. *Journal of Geophysical Research: Biogeosciences*, *116*(3), 1–19. doi:
10.1029/2010JG001545, 2011.

Tian, F., Wigneron, J. P., Ciais, P., Chave, J., Ogée, J., Peñuelas, J., Ræbild, A., Domec, J. C.,
Tong, X., Brandt, M., Mialon, A., Rodriguez-Fernandez, N., Tagesson, T., Al-Yaari, A.,
Kerr, Y., Chen, C., Myneni, R. B., Zhang, W., Ardö, J., & Fensholt, R.: Coupling of
ecosystem-scale plant water storage and leaf phenology observed by satellite. *Nature
1250   Ecology and Evolution*, *2*(9), 1428–1435. doi: 10.1038/s41559-018-0630-3, 2018.

Tuzet, A. J.: Stomatal Conductance, Photosynthesis, and Transpiration, Modeling. In J. Gliński,
J., Horabik, J., Lipiec (Ed.), Encyclopedia of Agrophysics. Encyclopedia of Earth Sciences
Series (pp. 855–858). Dordrecht. doi: 10.1007/978-90-481-3585-1_213, 2011.

Urban, J., Ingwers, M. W., McGuire, M. A., & Teskey, R. O.: Increase in leaf temperature opens
stomata and decouples net photosynthesis from stomatal conductance in Pinus taeda and
Populus deltoides x nigra. *Journal of Experimental Botany*, *68*(7), 1757–1767. doi:
10.1093/jxb/erx052, 2017.

Van Der Ent, R. J., Wang-Erlandsson, L., Keys, P. W., & Savenije, H. H. G.: Contrasting roles
of interception and transpiration in the hydrological cycle – Part 2: Moisture
1260   recycling. *Earth System Dynamics*, *5*(2), 471–489. doi: 10.5194/esd-5-471-2014, 2014.

Van Der Ent, Rudi J., Savenije, H. H. G., Schaefli, B., & Steele-Dunne, S. C.: Origin and fate of
atmospheric moisture over continents. *Water Resources Research*, *46*(9), 1–12. doi:
10.1029/2010WR009127, 2010.

Vinya, R., Malhi, Y., Brown, N. D., Fisher, J. B., Brodribb, T., & Aragão, L. E. O. C.: *Seasonal*

changes in plant – water relations in fl uence behaviours of leaf display in Miombo woodlands : evidence of water conservative strategies. Fuller 1999, 104–112. doi: 10.1093/treephys/tpy062, 2018.

WARMA.: *Catchments for Zambia*. Luangwa Catchment. Retrieved from http://www.warma.org.zm/catchments-zambia/luangwa-catchment-2/, 2022.

1270   Weerasinghe, I., Bastiaanssen, W., Mul, M., Jia, L., & Van Griensven, A.: Can we trust remote sensing evapotranspiration products over Africa. *Hydrology and Earth System Sciences*, *24*(3), 1565–1586. doi: 10.5194/hess-24-1565-2020, 2020.

Wehr, R., Commane, R., Munger, J. W., Barry Mcmanus, J., Nelson, D. D., Zahniser, M. S., Saleska, S. R., & Wofsy, S. C.: Dynamics of canopy stomatal conductance, transpiration, and evaporation in a temperate deciduous forest, validated by carbonyl sulfide uptake. *Biogeosciences*, *14*(2), 389–401. doi: 10.5194/bg-14-389-2017, 2017.

White, F.: *The vegetation of Africa*. Paris: UNESCO, 1983.

World Bank.: *A Multi-Sector Investment Opportunities Analysis*. Washington, D.C, 2010.

Zhang, K, Kimball, S. J., and Running, W.S.,: "A Review of Remote Sensing Based Actual
1280   Evapotranspiration Estimation." *Wiley Interdisciplinary Reviews: Water* 3 (6): 834–53. https://doi.org/10.1002/wat2.1168, 2016.

Zhao, M., Peng, C., Xiang, W., Deng, X., Tian, D., Zhou, X., Yu, G., He, H., & Zhao, Z.: Plant phenological modeling and its application in global climate change research: Overview and future challenges. *Environmental Reviews*, *21*(1), 1–14. doi: 10.1139/er-2012-0036, 2013.

Zimba, H. M., Coenders-gerrits, M. A. J., Banda, K. E., Schilperoort, B., Nyambe, I., van de Giesen, N., & Savenije, H. H. G.: Measuring evaporation across canopy phenophases of a natural forest : Miombo forest , Southern Africa. *Hydrol. Earth Syst. Sci. Discuss*, *October*, 1–23. doi: hthttps://doi.org/10.5194/hess-2022-303, 2022.

Zimba, H., Coenders-Gerrits, M., Kawawa, B., Savenije, H., Nyambe, I., & Winsemius, H.:
1290   Variations in canopy cover and its relationship with canopy water and temperature in the miombo woodland based on satellite data. *Hydrology*, *7*(3). doi: 10.3390/HYDROLOGY7030058, 2020.